Study on Shrinkage Properties of Repairing Mortar Modified by Basalt Fiber

S.Y. Yang[1,*], P.P. Xu[1]

[1]School of Civil Engineering and Water Conservancy, Ningxia University, Yinchuan 750021, PR China, yangshuyan@nxu.edu.cn (S.Y. Yang, Corresponding author), 1462552543@qq.com(P.P. Xu).

Abstract: *In order to study the shrinkage properties of modified repairing mortar, an orthogonal experiment with four factors and three levels were proceeded. Nine specimens with four factors, i.e., silica powder, sodium silicate, basalt fiber and a U-type expansive agent, were used to measure the length change ratio. The results show that the shrinkage value of modified repairing mortars have been greatly reduced. Compared with the control specimen without any additives, the shrinkage value of the modified repairing mortar with the silica powder of 3 %, the sodium silicate of 1.0 %, the basalt fiber of 0.2 % and the U-type expansive agent of 10 % at 60d drops by 42.5%. Based on experimental results, the shrinkage prediction model of modified repairing mortar has been established. The model can be used to predict the shrinkage value of the modified repairing mortar with similar compositions.*

Keywords: *Shrinkage properties; Repairing mortar; Basalt fiber; Orthogonal experiment; Prediction model.*

1 Introduction

Concrete damage has always been a common problem in concrete structures. In order to restore the function of damaged concrete structures, cement-based materials such as concrete or mortar have been usually used as repairing materials (Zailani et al. 2020, Yang et al. 2020, Xue et al. 2021, Oh et al. 2022). Cement-based material is one of the most widely used building materials in the world, which has both advantages, such as easy access of raw materials, easy production and construction, and disadvantages, like high shrinkage (Zhang et al. 2021), easy cracking (Szeląg 2020) and low compressive strength (Kasal and Vítek 2022). Those disadvantages will lead to certain safety risks when cement-based materials are used in repairing structures.

In the past decades, for the sake of improvement of those disadvantages, many scholars have adopted different modification methods to cement-based materials. Some researchers found that the shrinkage properties of cement-based materials are significantly improved after the addition of appropriate fibers, such as steel fiber (SF) (Al-musawi et al. 2019, Roberti et al. 2020), polypropylene (PP) fiber (Marushchak et al. 2022, Ma et al. 2022), basalt fiber (BF) (Punurai et al. 2018, Zheng et al. 2019). Some characters (Saje et al. 2013, Ma et al. 2017, George and Abin Thomas 2020) of fiber, like length, length-diameter ratio and the dosage of fiber, have great influence on the improvement of shrinkage. In the cement hardening stage, these fibers are evenly distributed in matrix and connected with plenty of the pores in the interior, which inhibit partial shrinkage cracks. After the cracking of matrix, fibers effectively alleviated the

stress at the microcracks in matrix (Vianna et al. 2022). and restrained the further propagation of microcracks by bridging some fracture interfaces.

As a repairing material, high compressive strength, low shrinkage, good bonding property and good ductility are very important characteristics. So far, there have been many research results on the modification properties of single fiber or mineral admixtures or expansion agents or mixed fibers and expansion agents. However, there are little studies on the properties of mortar modified by multiple additives. In this study, a repairing mortar was prepared by mixing silica powder, sodium silicate, basalt fiber and a UEA expansion agent in ordinary mortar. Before and after modification, its shrinkage rates at different ages were compared and analyzed. The shrinkage mechanism of the repairing materials under different components was also discussed. The results can be helpful to the preparation and the application of new modified mortar with low shrinkage and high early compressive strength.

2 Materials and Methods

2.1 Materials

Experimental work utilized Ordinary Portland Cement (OPC) with a strength grade of 52.5R. A silica powder, SiO_2 content was more than 90 % and 7d activity index was 110 %. Sodium silicate, density (Be/20℃) was 38.5 and modulus (SiO_2/ K_2O) was 3.3. Basalt fiber, diameter was 0.015 mm, length was 12 mm, aspect ratio was 800:1 and density were 2.65 g/cm^3. Natural river sand had fineness modulus of 2.78. A UEA expansion agent, had alkali content of 0.46 % and limiting shrinkage rates of 7 d in water and 21 d in air were 0.037 % and -0.013% respectively. Polycarboxylic acid superplasticizer, water reduction rate was greater than 30 %. Mixed water was tapping water.

In this experiment, orthogonal test method was used to design the mix ratio. L_9 (3^4) table of four-factor and three-level is shown in Table1. Four factors were silica powder (factor A), sodium silicate (factor B), basalt fiber (factor C) and a UEA expander (factor D). Where, the factors, A, B and D were the quality fraction and the equal quality were used to replace part of the cement. Factor C was the volume fraction and replaced partial cement with equal volume. In order to compare with 9 orthogonal groups, the control sample without any additives was also listed in the Table1.

2.2 Methods

In order to prevent fiber aggregation and clumping, basalt fiber was artificially scattered and stirred at low speed. The pouring process is shown in Fig.1.

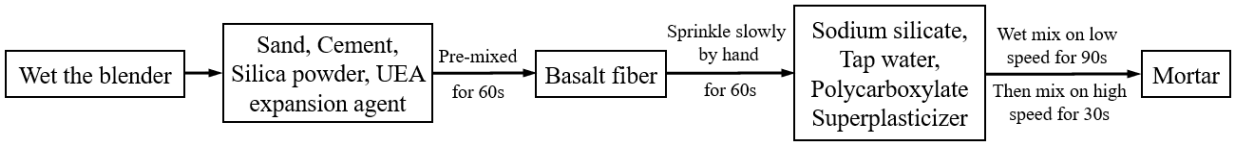

Figure 1. Pouring process of samples.

Table 1. Modified mortar mix ratio.

No.	Combination	Cement g/m^3	Silica powder (A)	Sodium silicate (B)	Basalt fiber (C)	UEA expansion agent (D)
S0	$A_0B_0C_0D_0$	400	0	0	0	0
S1	$A_1B_1C_1D_1$	354	3%(1)	0.5%(1)	0.1%(1)	8%(1)
S2	$A_1B_2C_2D_2$	344	3%(1)	1%(2)	0.2%(2)	10%(2)
S3	$A_1B_3C_3D_3$	334	3%(1)	1.5%(3)	0.3%(3)	12%(3)
S4	$A_2B_1C_2D_3$	326	6%(2)	0.5%(1)	0.2%(2)	12%(3)
S5	$A_2B_2C_3D_1$	340	6%(2)	1%(2)	0.3%(3)	8%(1)
S6	$A_2B_3C_1D_2$	330	6%(2)	1.5%(3)	0.1%(1)	10%(2)
S7	$A_3B_1C_3D_2$	322	9%(3)	0.5%(1)	0.3%(3)	10%(2)
S8	$A_3B_2C_1D_3$	312	9%(3)	1%(2)	0.1%(1)	12%(3)
S9	$A_3B_3C_2D_1$	326	9%(3)	1.5%(3)	0.2%(2)	8%(1)

The size of the shrinkage test specimen was 40 × 40 ×160 (mm), which was made in accordance with Standard of Test Method for Basic Properties of Building Mortar (JGJ/T70: 2009). Each group of samples had 3 pieces. Metal probes were embedded at both ends before pouring. After pouring and vibrating, the samples were covered with plastic films for 3d in standard curing room (20±2℃, >95%), and then the molds were removed. After marking direction, the samples were moved into a curing box with constant temperature and constant humidity (20±2℃, 90%). The initial length was measured 4 h later, and then the length was measured after *t* days (1, 3, 7, 14, 28, 45, 60, 90, 180 (d). The shrinkage rate ε_t of the specimens at *t* days was calculated as,

$$\varepsilon_t = (l_0 - l_t) / (l - l_d) \quad (1)$$

where, *l* was the original length of the sample and *l*=160 mm; l_d was the sum of buried lengths of the metal probes at both ends and l_d=20±2(mm); l_0 was the initial length after it was moved into the curing box for 4h; l_t was the length of the sample in the curing box for *t* days.

3 Results

3.1 Shrinkage Rate

Fig. 2 shows the shrinkage curves of the control sample S0 and orthogonal groups S1~S9 with the changes in age. As can be seen from Fig.2, the shrinkage rates of specimens in the orthogonal group had been significantly improved compared with that in the control sample. The shrinkage rate of all specimens increased with the increase of age, and the growth trend

was basically the same. The shrinkage rate increased rapidly within 28d, reaching more than 80%~90% of the maximum shrinkage rate. After 28 days, the growth rate of shrinkage slowed down and was basically stable after 60 days. The shrinkage rate of the control sample S0 was 749×10^{-6} at 60 days, which was the largest among the 10 groups of specimens. At 60 days, the shrinkage rate of S3($A_1B_3C_3D_3$) was 669×10^{-6}, which was 10.68 % lower than the control sample, but was the highest among the 9 orthogonal groups. The shrinkage rate of S2 ($A_1B_2C_2D_2$) was 431×10^{-6}, which was the smallest in the 9 orthogonal groups and 42.5 % lower than the control sample. From 60d to 180d, the shrinkage rate of mortars changed very little.

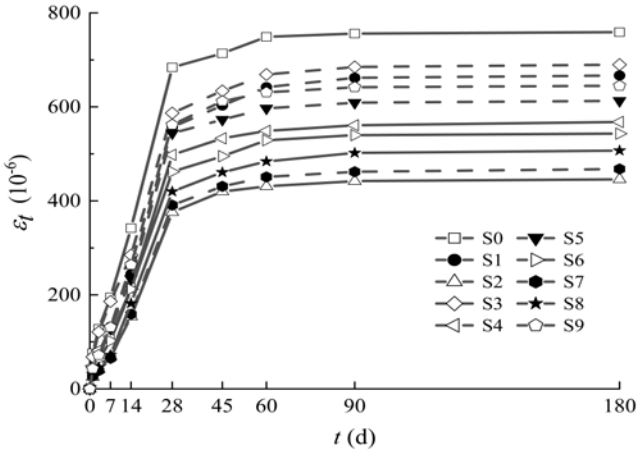

Figure 2. Shrinkage rate curves with the increase of ages.

Range analysis is a normally analysis method of orthogonal test results. By calculating the mean value of deviation under different levels of each factor, the optimal level and the worst level of each factor can be identified. Based on the calculation result, the range value $R = k_{max} - k_{min}$ of each factor can be obtained. R indicates the influence degree of the corresponding factor on the test index. Thus, the ranking of influencing factors of the index can be obtained. Table 2 shows the range values R of factors A, B, C and D under the shrinkage index of 3 days, 28 days, 60 days and 180 days.

Table 2. Range R of shrinkage at different ages.

R	Silica powder (A)	Sodium silicate (B)	Basalt fiber (C)	UEA expansion agent (D)	Order
3d	13.3	22.2	11.6	15.3	B > D > A > C
28d	49.0	90.3	28.7	144.7	D > B > A > C
60d	51.0	95.7	26.3	147.3	D > B > A > C
180d	61.0	104.0	37.3	156.0	D > B > A > C

For mortar, the shrinkage rate is negative index, that is, the smaller the shrinkage rate, the better the shrinkage performance of modified mortar. As shown in Table 2, factor B (sodium silicate) was the main influencing factor of 3d shrinkage rate. Factor D (UEA expander content) was the main influencing factors of index 28d, 60d and 180d shrinkage rate. Factor C (basalt fiber) had the least effect on early and late shrinkage rate, while factor A (silica powder) had more effect. UEA expander replaced part of cement, greatly reducing the shrinkage of cement in the processing of setting and hardening. In addition, the expander itself reacted with some components in the cement to produce ettringite and Ca $(OH)_2$ with a slight expansion effect, compensating for part of the shrinkage deformation generated by the matrix (Wu et al. 2022). Silica powder replaced parts of cement, which reduced the chemical shrinkage of cement slurry. On the other hand, the small particle size and large specific surface area of silica powder improved the appropriate amount of incorporation into the cement matrix and the overall compactness. Under the condition of relatively constant ambient humidity, the water loss of dense cement matrix was less, and the shrinkage deformation was relatively reduced (Yu et al. 2021). The addition of basalt fiber can obviously optimize the shrinkage property of mortar, and formed a three-dimensional chaotic support system in the matrix by the fiber and then reduced the particle subsidence in the cement matrix, which improved the compactness and fluidity of the matrix to a certain extent, and was conducive to the reduction of shrinkage deformation (Ma et al. 2017) . When the basalt fiber was overmixed, it was easy to form partial clumping in the cement matrix, which affected its workability and bleeding capacity, then increased the shrinkage deformation of the modified mortar (Hu and Xia 2022).

3.2 Prediction Model of Shrinkage Rate of Modified Mortar

Based on the experimental results and range analysis of the shrinkage rate, orthogonal factors have a great influence on the shrinkage rate. A shrinkage prediction model of modified mortar was established based on test results, data dispersion degree and dynamic development characteristics of shrinkage index. Based on the experimental results, a fitting formula of shrinkage rate ε_t at t days is proposed as,

$$\varepsilon_t = c_0 + ae^{(-t/b)} \qquad (2)$$

where, a, b and c_0 were regression coefficients. The least square method was used to compare Equ. (2) and experimental results, and the fitting parameters are shown in Table 3. R^2 in the table were all greater than 0.96, indicating that the formula has a good fitting.

Multiple nonlinear regression analysis was carried out by Design-Expert 8.0 software. The quadratic polynomial regression model of three parameters (a, b, c_0) and four factors (A, B, C, D) was obtained. The formulas of regression coefficients are listed in Equ. (3) ~ (5).

Table 3. Fitting parameters of modified mortar.

No.	Fitting parameters			R^2
	a	b	c_0	
S1	-698.71	22.52	685.21	0.9773
S2	-479.88	22.64	462.32	0.9681
S3	-694.81	20.72	703.88	0.9821
S4	-591.29	21.31	584.20	0.9678
S5	-648.75	20.77	631.48	0.9713
S6	-571.99	21.73	558.75	0.9772
S7	-503.66	23.19	484.08	0.9674
S8	-540.35	23.16	522.38	0.9716
S9	-683.20	20.55	665.50	0.9768

$$a = -270.47B^2 - 31.09D^2 - 18.37BD + 5.06A + 672.56B + 657.10D - 4.18\times10^3 \quad (3)$$

$$b = 0.10A^2 - 0.25D^2 + 0.17AD - 2.82A - 0.31B + 0.63C + 4.15D + 9.08 \quad (4)$$

$$c_0 = 299.51B^2 + 32.60D^2 + 19.87BD - 6.66A - 739.46B - 686.14D + 4.33\times10^3 \quad (5)$$

where, A, B, D represented the equality fraction replacing cement of silica powder, sodium silicate, and UEA expander respectively and C represented volume fraction of basalt fiber. The unit were %.

The comparisons between the models and experimental results are shown in Fig.3. It can be seen from Fig. 3 that the linear proximity between the predicted points and the actual points are very well, indicating that the correlations are strong without significant difference. It is further indicated that the model can be used to analyze and predict the shrinkage rate of modified mortar.

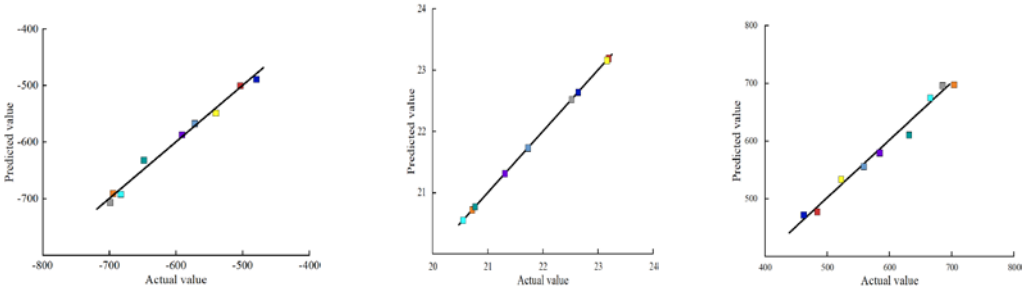

(a) （b） （c）

Figure 3. Comparison between predicted value and actual value of the regression model (a) a; (b) b; (c) c_0.

4 Conclusion

Based on the experimental results and analysis, the shrinkage characteristic of the repairing mortar modified by basalt fiber and other additives at the ages of 1 to 180 days can be drawn:
1) The shrinkage trends of the control sample and the modified orthogonal groups increased with the increase of age and had a similar rule. The shrinkage deformation mainly occurred within 28 days, reaching 80% ~ 90% of the total deformation. The growth rate of shrinkage deformation slowed down after 28 days, and basically kept stable after 60 days until 180 days.
2) After modification, the shrinkage property of mortar at 60 days was greatly improved and the best group reduced by 42.5 % than the control sample.
3) Through the fitting and the multiple nonlinear regression analysis of experimental results, a new prediction model of shrinkage rate of modified mortar was established, i.e., $\varepsilon_t = c_0 + a\mathrm{e}^{-t/b}$.

The model can be used to predict the shrinkage rate of modified mortar with similar materials.

Acknowledgements

The authors gratefully acknowledge the financial support from National Natural Science Foundation of China (Grant No. 51868065).

References

Al-musawi, H., Figueiredo, F.P., Guadagnini, M., Pilakoutas, K. (2019). *Shrinkage properties of plain and recycled steel–fibre-reinforced rapid hardening mortars for repairs*. Construction and Building Materials, 197, 369.

George, A., Abin Thomas, C.A. (2020). *Influence of Alkali Resistant Glass Fiber on the Reduction of Plastic Shrinkage Cracking of Self Compacting Concrete*. Proceedings of SECON 2020: Structural Engineering and Construction Management 4, 325-334.

Hu, X., Xia, K. (2022). *Experimental study on the permeability of basalt fiber engineered cementitious composite (ECC)*. Materials and Structures, 55(2):85.

JGJ/T 70 (2009). Standard test method for basic properties of building mortar.

Kasal, P., Vítek, J.L. (2022). *The Effect of Cement Mortar Recipe on Early Age Strength Development*. Solid State Phenomena, 336,179-184.

Marushchak, U., Sydor, N., Margal, I. (2022). *Impact of Polypropylene Fibers on the Properties of Engineered Cementitious Composites*. Proceedings of EcoComfort 2022.

Ma, L., Zhang, Q., Lombois-Burger, H., Jia, Z., Zhang, Z., Niu, G., Zhang, Y. (2022). *Pore structure, internal relative humidity, and fiber orientation of 3D printed concrete with polypropylene fiber and their relation with shrinkage*. Journal of Building Engineering, 61,105250.

Ma, R., Yang, J., Liu, Y., Zheng, X. (2017). *Influence of length-to-diameter ratio on shrinkage of basalt fiber concrete*. IOP Conference Series: Materials Science and Engineering, 242(1),012027.

Oh, S.R., Lee, K.M., Choi, S., Choi, Y.W. (2022). *Fundamental Properties and Self-Healing Performance of Repair Mortar with Solid Capsules Made Using Inorganic Reactive Powder*, Materials, 15(5), 1710.

Punurai, W., Kroehong ,W., Saptamongkol, A., Chindaprasirt, P. (2018). *Mechanical properties, microstructure and drying shrinkage of hybrid fly ash-basalt fiber geopolymer paste*, Construction and Building Materials, 186, 62-70.

Roberti, F., Cesari, V.F., Matos P.R., Pelisser, F., Pilar, R. (2020). *High- and ultra-high-performance concrete produced with sulfate-resisting cement and steel microfiber: Autogenous shrinkage, fresh-state, mechanical properties and microstructure characterization*, Construction and Building Materials, 121092.

Szeląg, M. (2020). *Evaluation of Cracking Patterns in Cement Composites—From Basics to Advances: A Review*, Materials, 13(11), 2490.

Saje, D., Bandelj, B., Šušteršic, J. (2013). *Shrinkage and Creep of Steel Fiber Reinforced Normal Strength Concrete*, ASTM International.

Vianna, N.J., Silva ,Forti, N.C., Moraes, G.P., Silva, J.B. (2022). *Drying Shrinkage of Fiber Reinforced Concrete Under Restrained Conditions: A Systematic Mapping Study*, Proceedings of the 7th Brazilian Technology Symposium on Emerging Trends in Systems Engineering Mathematics and Physical Sciences BTSym2021.

Wu, L., Yu, Z., Zhang, C., Zhen, Y., Toshiyuki, B. (2022). *Shrinkage and tensile properties of ultra-high-performance engineered cementitious composites (UHP-ECC) containing superabsorbent polymers (SAP) and united expansion agent (UEA)*, Construction and Building Materials, 339,127697.

Xue, S., Meng, F., Zhang, P., Wang, J., Bao, J., He, L. (2021). *Influence of substrate moisture conditions on microstructure of repair mortar and water imbibition in repair-old mortar composites*, Measurement, 183, 109769.

Yu, Z., Zhao, Y., Ba, H., Liu, M. (2021). *Relationship between buck electrical resistivity and drying shrinkage in cement paste containing expansive agent and mineral admixtures*, Journal of Building Engineering, 39,102261.

Yang, J., Wang, R., Zhang, Y. (2020). *Influence of dually mixing with latex powder and polypropylene fiber on toughness and shrinkage performance of overlay repair mortar*, Construction and Building Materials, 261(5), 120521.

Zailani, W.W.A., Abdullah, M.M.A.B., Arshad, M.F., Razak, R.A., Tahir, M.F.M., Zainol, R.R.M.A., Nabialek, M., Sandu, A.V., Wysłocki, J.J., Błoch, K. (2020). *Characterisation at the Bonding Zone between Fly Ash Based Geopolymer Repair Materials (GRM) and Ordinary Portland Cement Concrete (OPCC)*, Materials, 14(1): 56.

Zhang, M., Aba M., Sakoi, Y., Tsukinaga, Y., Shimomukai ,K., Kuang, Y. (2021). *Synergetic Effect of Expansive Agent (KEA) and Superabsorbent Polymers (SAP) on the Shrinkage, Strength and Pore Structures of Mortar*s, Journal of Advanced Concrete Technology, 19(1), 26-39.

Zheng, Y., Zhang, P., Cai, Y., Jin, Z., Moshtagh, E. (2019). *Cracking resistance and mechanical properties of basalt fibers reinforced cement-stabilized macadam*, Composites Part B, 165, 312-334.